SEMARAK ILMU PUBLISHING

Journal of Advanced Research in Numerical Heat Transfer

Journal homepage:
https://semarakilmu.com.my/journals/index.php/arnht/index
ISSN: 2735-0142

Stagnation-Point Flow and Heat Transfer over an Exponentially Stretching/Shrinking Inclined Plate in a Micropolar Fluid

Fairul Naim Abu Bakar[1], Siti Khuzaimah Soid[1,*], Nur Hazirah Adilla Norzawary[2], Farizza Haniem Sohut[3]

[1] Faculty of Computer and Mathematical Sciences, Universiti Teknologi MARA (UiTM), 40450 Shah Alam, Selangor, Malaysia
[2] Institute for Mathematical Research, Universiti Putra Malaysia (UPM), 43400 Serdang, Selangor, Malaysia
[3] Department of Mathematical Sciences, Universiti Kebangsaan Malaysia (UKM), 43600 Bangi, Selangor, Malaysia

ARTICLE INFO

Article history:
Received 21 October 2023
Received in revised form 19 November 2023
Accepted 20 December 2023
Available online 31 January 2024

Keywords:
Micropolar fluid; heat transfer; exponentially stretching/shrinking; inclined plate; MHD; radiation; concentration

ABSTRACT

The study investigates the fluid flow characteristics and heat transfer over an exponentially stretching/shrinking inclined plate immersed in a micropolar fluid. The micropolar fluid model considers the rotational effects of microelements relevant to complex industrial fluid behavior. Using similarity variables, the governing equations for fluid flow and heat transfer are transformed from Partial Differential Equations (PDEs) to Ordinary Differential Equations (ODEs), and appropriate boundary conditions are incorporated to simulate the behavior of the micropolar fluid over the inclined plate. The ODEs are numerically solved using MATLAB software with BVP4c, and the results are compared with previous findings, showing good agreement. The effects of critical parameters such as plate inclination angle, stretching/shrinking rate, and micropolar fluid parameters are examined. Notably, the micropolar parameter significantly influences the skin friction for stretching and shrinking flows. An increase in the micropolar parameter leads to increased skin friction for stretching flows, while for shrinking flows, the skin friction decreases within a specific range of stretching/shrinking values. The behavior of the local couple stress becomes complex as the micropolar parameter increases. Additionally, the local Nusselt number decreases as the micropolar parameter increases for shrinking flows, indicating a reduction in heat transfer from the solid surface during shrinking flow. Moreover, an increase in the Sherwood number suggests a relatively slower mass transfer rate than momentum transfer. These findings offer valuable insights into the behavior of micropolar fluids over exponentially stretching/shrinking inclined plates, guiding optimizing heat transfer and fluid flow in practical engineering systems.

1. Introduction

1.1 Research Background

The study focuses on a micropolar fluid's flow and heat transfer characteristics over an exponentially stretching/shrinking inclined plate, emphasizing the stagnation-point region. Magneto-Hydro Dynamic (MHD), radiation, and concentration are also considered. Micropolar fluids exhibit

* *Corresponding author.*
E-mail address: khuzaimah@tmsk.uitm.edu.my (Siti Khuzaimah Soid)

https://doi.org/10.37934/arnht.16.1.1734

unique behavior due to additional microstructural properties, such as rotations and higher-order gradients. Stagnation-point flow and heat transfer phenomena are of significant interest in fluid dynamics and heat transfer research due to their wide applications in various engineering and industrial processes. The exponentially stretching/shrinking plate offers variable deformation effects, making it an interesting case for investigation.

The study formulates and solves the governing equations for micropolar fluid flow and energy transfer. Exploring the complex interplay between micropolar fluid effects, plate deformation, and inclination angle will be interpreted using graphs. Similarity variables were employed to turn the governing partial differential equations (PDEs) into ordinary differential equations (ODEs). The amended equations were then numerically solved in MATLAB using BVP4c. The outcomes of this research have potential applications in advanced cooling techniques, materials processing, and boundary-layer control strategies in non-Newtonian fluid systems.

While significant progress has been made in the study of micropolar fluid dynamics, stagnation-point flow, and heat transfer over various types of surfaces, there exists a notable research gap in understanding the combined effects of micropolar fluids, magnetohydrodynamics (MHD), radiation, and concentration over an exponentially stretching/shrinking inclined plate in the stagnation-point region. The literature review reveals that previous studies have often focused on individual aspects, such as micropolar fluids or exponentially stretching plates. However, they have yet to explore the intricate interplay between these factors comprehensively.

Furthermore, understanding micropolar fluid behavior in complex geometries provides insights into fundamental aspects of fluid dynamics and heat transfer in non-Newtonian systems, contributing to the broader knowledge in this interdisciplinary field. The results gained will be beneficial for applications and as a supplement to prior research.

1.2 Micropolar Fluid

Micropolar fluid is a non-Newtonian fluid that exhibits additional microstructural effects that influence its flow behavior, such as spinning particles, the rotation of which is defined by an independent microrotation vector [1]. These fluids can be utilized to study the behavior of exotic lubricants, animal blood, polymer fluids, dust clouds, river sediments, and liquid crystals containing rigid molecules [2].

The concept of micropolar fluid dynamics was first introduced in the mid-20th century by Eringen [3]. Since then, researchers have significantly advanced micropolar fluid dynamics' theoretical formulation and practical applications. Ishak *et al.,* [4] studied a micropolar fluid's steady two-dimensional stagnation-point flow over a shrinking sheet. The shrinking and ambient fluid velocities are assumed to vary linearly with the distance from the stagnation point. While, Norzawary *et al.,* [5] investigated stagnation point flow of MHD micropolar hybrid nanofluids over a deformable sheet with viscous dissipation with stability analysis. They concluded that non-unique solutions exist for the phenomenon of shrinking sheets. The studies of micropolar fluid were extended in numerous ways, such as [6-12].

Understanding micropolar fluid has practical applications. Micropolar fluids' unique characteristics present new flow optimization and control possibilities in engineering devices.

1.3 Stagnation-point Flow and Heat Transfer

Stagnation-point flow describes the fluid motion around the stagnation area at the front of a blunt-nosed body, shown by all solid bodies moving in a fluid. The stagnation area has the highest

pressure, heat transmission, and mass deposition rates. Stagnation point flow is evident in an airfoil's aerodynamics, where its movement through the air impacts the air flow around its leading edge due to a stagnation point. Stagnation point flow is crucial in various engineering and scientific applications, influencing design decisions, performance optimization, and fundamental understanding of fluid behavior.

Heat transfer is a significant technological challenge in various industrial and engineering applications. Heat transfer, which involves the movement of energy from one part to another due to temperature differences, is a crucial aspect of these processes [13]. Fluid movement is vital in many industrial operations, especially those requiring efficient heat transfer. A fluid is often employed to extract heat from its source during the heat transfer. As a result of the temperature difference between the surface and the fluid in the system, a thermal boundary layer is formed. Heat naturally flows from regions of high temperature to those of lower temperature, making understanding and managing heat transfer essential in various technological applications.

In various industries, there are numerous practical uses for stagnation point flow combined with heat transfer over a surface that is either stretching or shrinking. Bhattacharyya *et al.,* [14], have expanded the study on this flow and heat transfer type. They specifically explored how the slip effect influences the boundary layer stagnation-point flow and heat transfer over a shrinking sheet. Their work contributes valuable insights to this fascinating field of research. It finds use in various areas such as managing the boundary layer along material handling conveyors, understanding blood flow challenges, improving aerodynamics, plastic sheet manufacturing, cooling metallic plates in a bath, and optimizing processes in textile and paper industries, among others. The study of this flow phenomenon plays a crucial role in enhancing efficiency and performance across different industrial sectors. Several recent studies, including those conducted by Dzulkifli *et al.,* [15], Japili *et al.,* [16], Ismail *et al.,* [17], and Vishalakshi *et al.,* [18], have contributed to the understanding of stagnation-point flow and heat transfer. These works represent significant extensions and advancements in the field.

1.4 Exponentially Stretching/Shrinking Inclined Plate

Exponentially stretching/shrinking inclined plates have been a subject of interest in fluid mechanics and heat transfer due to their relevance in various engineering and industrial applications. Researchers have recently investigated fluids' flow and heat transfer characteristics over such plates [19-21].

The exponentially stretching/shrinking plate provides an exciting and practical case for exploration. It offers a variable stretching or shrinking parameter, allowing researchers to examine various deformation effects on the flow and heat transfer characteristics. Furthermore, the inclination of the plate introduces additional complexities, affecting the flow separation, recirculation zones, and thermal boundary layer development.

The findings from these studies have applications in various engineering fields, such as aerospace, manufacturing, chemical processing, and renewable energy, where heat transfer optimization is critical for performance enhancement and system design.

2. Mathematical Formulation

In this study, we delve into the graceful movement of a micropolar fluid toward a stagnation point on an inclined plate, as illustrated in Figure 1. The plate is elegantly set at an acute angle, α , with the x and y axes serving as the backdrop. Amidst this journey, the fluid is propelled by a constant

free stream velocity, $u_e(x) = ae^{x/L}$ where $a > 0$ (constant) and accompanied by the touch of a reference length, L. A dance of expansion and contraction ensues, with $u_w(x) = be^{\frac{x}{L}}$ denoting the exponential velocity for stretched $(b > 0)$ or shrunk $(b < 0)$ surfaces, while $b = 0$ gracefully embodying the static surface's essence. The surface temperature is given as $T_w(x) = T_\infty + T_0 e^{\frac{2x}{L}}$ where T_0 is a constant and T_∞ is the ambient temperature. The concentration on the surface is $C_w(x) = C_\infty + C_0 e^{\frac{2x}{L}}$ where C_0 is a constant and C_∞ ambient concentration. Hence, g is a symbol of acceleration due to gravity.

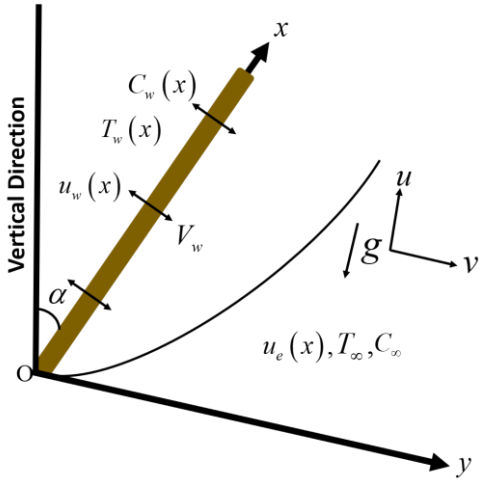

Fig. 1. Physical Model

This study focuses exclusively on the behavior of a micropolar fluid as it encounters a stagnation point over an inclined plate that is exponentially either stretching or shrinking. This analysis includes the influence of radiation, magnetohydrodynamics (MHD), mixed convection, and radiation effects. The study further presents solutions for specific parameter values related to stretching, shrinking, and buoyancy-assisted or opposing flow direction. The fundamental governing equations for the boundary layer are a set of parabolic partial differential equations (PDEs) encompassing continuity, linear momentum, angular momentum, energy, and concentration equations.:

Continuity equation

$$\frac{\partial u}{\partial x} + \frac{\partial v}{\partial y} = 0 \tag{1}$$

Linear momentum equation

$$u\frac{\partial u}{\partial x} + v\frac{\partial u}{\partial y} = u_e\frac{du_e}{dx} + \left(\upsilon + \frac{\kappa}{\rho}\right)\frac{\partial^2 u}{\partial y^2} + \frac{\kappa}{\rho}\frac{\partial N}{\partial y} + g\left[\beta_T\left(T - T_\infty\right) + \beta_c\left(C - C_\infty\right)\right]\cos\alpha - \frac{\sigma B^2}{\rho}\left(u - u_e\right) \tag{2}$$

Angular momentum equation

$$u\frac{\partial N}{\partial x} + v\frac{\partial N}{\partial y} = \frac{\chi}{\rho j}\frac{\partial^2 N}{\partial y^2} - \frac{\kappa}{\rho j}\left(2N + \frac{\partial u}{\partial y}\right) \tag{3}$$

Energy equation

$$u\frac{\partial T}{\partial x}+v\frac{\partial T}{\partial y}=\frac{k}{\rho c_p}\frac{\partial^2 T}{\partial y^2}-\frac{1}{\rho c_p}\frac{\partial q_r}{\partial y} \tag{4}$$

Concentration equation

$$u\frac{\partial C}{\partial x}+v\frac{\partial C}{\partial y}=D\frac{\partial^2 C}{\partial y^2} \tag{5}$$

The boundary requirements must be satisfied at all points along the boundary of a region for a set of differential conditions to be solved. The boundary conditions applicable to the flow are:

$$u=u_w=be^{x/L},\ v=0,\ T=T_w=T_\infty+T_0e^{2x/L},\ N=-m\frac{\partial u}{\partial y},\ C=C_w=C_\infty+C_0e^{2x/L}\ \text{at}\ y=0$$
$$u\to u_e,\ T\to T_\infty,\ N\to 0,\ C\to C_\infty\ \text{as}\ y\to\infty \tag{6}$$

Imagine considering the velocities in two directions: one along the x-axis and the other along the y-axis. In this scenario, the symbol $\upsilon=\mu/\rho$ represents the kinematic viscosity, ρ stands for fluid density, μ is the fluid viscosity coefficient, N represents microrotation or angular velocity, $j=2L\upsilon e^{-x/L}/a$ is micro-inertia per unit mass, $\chi=\mu\left(1+K/2\right)j$ represents spin gradient, and κ is vortex viscosity. The fluid's electrical conductivity is denoted as σ, and we have a varying magnetic field denoted as $B\left(x\right)=B_0e^{x/2L}$, where B_0 is a constant. Additionally, c_p represents the specific heat of the fluid, and β_T, β_C are the coefficients represent thermal and concentration expansion, respectively. To simplify the equations from (1) to (5), including the boundary condition in Eq. (6), we can introduce a similarity transformation:

$$\eta=\sqrt{\frac{a}{2\upsilon L}}e^{\frac{x}{2L}}y,\quad u=ae^{\frac{x}{L}}f'(\eta),\quad v=-\sqrt{\frac{a\upsilon}{2L}}e^{\frac{x}{2L}}\left(f(\eta)+\eta f'(\eta)\right),\quad \theta(\eta)=\frac{T-T_\infty}{T_w-T_\infty}$$
$$N=a\sqrt{\frac{a}{2\upsilon L}}e^{\frac{3x}{2L}}h(\eta),\quad \phi=\frac{C-C_\infty}{C_w-C_\infty} \tag{7}$$

where η is the similarity variable, while u and v denotes the stream function that the continuity Eq. (1) is identically fulfilled. Thus, the transformed linear momentum Eq. (2), angular momentum Eq. (3), energy Eq. (4) and concentration Eq. (5) become:

$$\begin{aligned}
&(1+K)f''' + ff'' - 2(f')^2 + 2 + Kh' + 2\lambda\left(\theta(\eta) + \delta\phi(\eta)\right)\cos\alpha - M(f'-1) = 0\\
&\left(1+\frac{K}{2}\right)h'' - K(2h + f'') + fh' - 3f'h = 0\\
&\frac{1}{\Pr}\left[1+\frac{4}{3}R\right]\theta'' + f(\eta)\theta'(\eta) - 4f'(\eta)\theta(\eta) = 0\\
&\frac{1}{Sc}\phi'' + f\phi' - 4f'\phi = 0
\end{aligned} \tag{8}$$

The corresponding boundary conditions:

$$\begin{aligned}
&f'(0) = \frac{b}{a} = \varepsilon, \quad f(0) = 0, \quad \theta(0) = 1, \quad h(0) = -mf''(0), \quad \phi(0) = 1 \text{ at } \eta = 0\\
&f'(\eta) \to 1, \quad \theta(\eta) \to 0, \quad h(\eta) \to 0, \quad \phi(\eta) \to 0 \text{ as } \eta \to \infty
\end{aligned} \tag{9}$$

where the prime indicates differentiation concerning and $M = 2\sigma B_0^2 L / \rho a$ is Hartmann number or magnetic parameter. $\lambda = g\beta_T T_0 L / a^2$ is buoyancy parameter, $\delta = \beta_c C_0 / \beta_T T_0$ is constant concentration buoyancy parameter, α is an angle for inclined plate parameter, $\varepsilon = b / a$ is the stretching/shrinking parameter. Next, $K = \kappa / \mu$, $\Pr = \mu c_p / k$, $R = 4\sigma^* T_\infty^3 / k^*$, and $Sc = \upsilon / D$ are the micropolar parameter, Prandtl number radiation, and Schmidt number parameters, respectively.

The involved physical quantities are the skin friction coefficient C_f, the local Nusselt number Nu_x, the local couple stress M_x and the local Sherwood number Sh_x [22]:

$$C_f = \frac{\tau_w}{\rho u_e^{\,2}}, \quad M_x = \frac{\chi\left(\frac{\partial N}{\partial y}\right)_{y=0}}{\rho x u_e^{\,2}}, \quad Nu_x = -\frac{xk}{k(T_w - T_\infty)}\left(\frac{\partial T}{\partial y}\right)_{y=0}, \quad Sh_x = -\frac{x}{(C_w - C_\infty)}\left(\frac{\partial C}{\partial y}\right)_{y=0} \tag{10}$$

Using the similarity variables Eq. (7) then,

$$\begin{aligned}
&C_f (\mathrm{Re}_x)^{1/2}\sqrt{\frac{2L}{x}} = \left[1+(1-m)K\right]f''(0), \quad M_x \mathrm{Re}_x = \left(1+\frac{K}{2}\right)h'(0),\\
&Nu_x (\mathrm{Re}_x)^{1/2}\sqrt{\frac{2L}{x}} = -\theta'(0), \quad Sh_x (\mathrm{Re}_x)^{1/2}\sqrt{\frac{2L}{x}} = -\phi'(0)
\end{aligned} \tag{11}$$

2. Mathematical Formulation

The transformed governing boundary layer equations have been efficiently tackled through numerical solutions utilizing the BVP4c function in MATLAB. The interplay of micropolar effects, stretching/shrinking phenomena, and inclination plate factors is elegantly brought to light through graphical representations of velocity, angular velocity, temperature, and concentration profiles.

Intriguing insights emerge as the skin friction coefficient $C_f\left(\mathrm{Re}_x\right)^{1/2}\sqrt{2L/x}$, the local couple stress $Nu_x\left(\mathrm{Re}_x\right)^{1/2}\sqrt{2L/x}$, the local Nusselt number (a measure of heat transfer rate) $M_x\,\mathrm{Re}_x$, and the local Sherwood number (an indicator of mass transfer rate) $Sh_x\left(\mathrm{Re}_x\right)^{1/2}\sqrt{2L/x}$, gracefully evolve. This captivating dance of parameters unfolds across various combinations of micropolar, and inclination angle attributes. Radiation, magnetic, Schmidt number and concentration buoyancy parameters are fixed and considered in this study.

The culmination of this exploration is aptly captured in Table 1 and Table 2, where a harmonious comparison of the skin friction coefficient $C_f\left(\mathrm{Re}_x\right)^{1/2}\sqrt{2L/x}$ and the local Nusselt number $Nu_x\left(\mathrm{Re}_x\right)^{1/2}\sqrt{2L/x}$ is artfully presented. The results from Soid *et al.,* [22] and Waini *et al.,* [19] are thoughtfully juxtaposed with the findings of the present study, creating a rich tapestry of insights.

Table 1

Comparison of Numerical Values $C_f\left(\mathrm{Re}_x\right)^{1/2}\sqrt{\frac{2L}{x}}$ for $\varepsilon=-0.5,0,0.5$

ε	Waini *et al.,* [18]	Soid *et al.,* [21]	Present Study
-0.5	2.1182	2.1182	2.1182
0	1.6872	1.6872	1.6872
0.5	0.9604	0.9604	0.9604

Table 2

Comparison of Numerical Values $Nu_x\left(\mathrm{Re}_x\right)^{1/2}\sqrt{\frac{2L}{x}}$ for $\varepsilon=-0.5,0,0.5$

ε	Waini *et al.,* [18]	Soid *et al.,* [21]	Present Study
-0.5	0.0588	0.0588	0.0588
0	2.5066	2.5066	2.5066
0.5	4.0816	4.0816	4.0816

The comparisons of the values in Tables 1 and 2, observed that the present results show an excellent agreement with the previous study. Therefore, this verifies the reliability and accuracy of the method used for this study. It is observed that the values of $C_f\left(\mathrm{Re}_x\right)^{1/2}\sqrt{2L/x}$ decreases but the values of $Nu_x\left(\mathrm{Re}_x\right)^{1/2}\sqrt{2L/x}$ increases when $\varepsilon=-0.5$.

3. Result

It's worth noting that while we're delving into the intricacies of these parameters, we're keeping other aspects constant. For instance, material properties $m=0.5$, and the Prandtl number $\mathrm{Pr}=6.2$, magnetic $M=2$, concentration buoyancy $\delta=1$, and the Schmidt number $Sc=0.2$ will remain steady in our analysis. This approach allows us to isolate the specific effects of the parameters we're studying.

The effects of K on the $C_f\left(\mathrm{Re}_x\right)^{1/2}\sqrt{2L/x}$, $M_x\,\mathrm{Re}_x$, $Nu_x\left(\mathrm{Re}_x\right)^{1/2}\sqrt{2L/x}$, and $Sh_x\left(\mathrm{Re}_x\right)^{1/2}\sqrt{2L/x}$ are presented in Figures 2-5, respectively for varies values of $K=0,0.5,1$. Figure 2 shows that when the plate shrinks, the skin friction coefficient decreases, while on a stretching plate, it increases. This change is due to the micropolar parameter becoming more prominent. On the shrinking plate, a larger micropolar parameter brings a more significant drop in

the skin friction coefficient. This implies that the microstructural characteristics play a more substantial role, causing less resistance on a shrinking plate. In contrast, a higher micropolar parameter on a stretching plate leads to a more noticeable rise in the skin friction coefficient. It suggests that the microstructural effects create a livelier interaction between the fluid and the surface, increasing resistance on a stretching plate. It also shows the transition from increase to decrease at the range between 1 and 1.5, that the skin friction is approximately zero (no drag force). The micropolar parameter intensifies the influence of microstructure on how fluid and surface interact, leading to distinct trends in skin friction for different flow scenarios of stretching and shrinking.

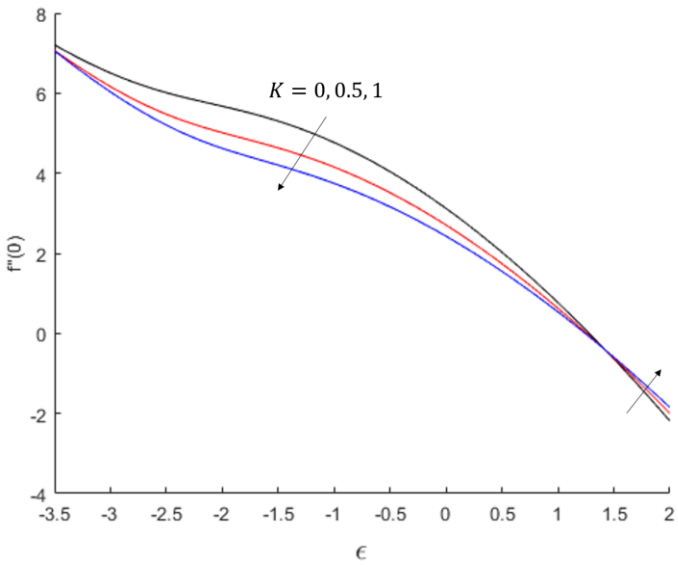

Fig. 2. $C_f \left(\mathrm{Re}_x\right)^{1/2} \sqrt{2L / x}$ for varies of *K*

Next, Figure 3 shows that an increase in the value of the micropolar parameter leads to an increase in the local couple stress. The couple stress is related to a particle rotational speed gradient on the surface. It also shows that the local couple's stress decreases between -1.5 and 1.5 and increases again due to the stretch. When the values of the surface shear stress and the local couple stress are zero, in terms of physics, zero surface shear stress occurs when the fluid and solid surfaces move at the same speed, resulting in no friction at the fluid-solid interface. While the couple stress is zero, it may be due to the non-effect of micro-structure, which causes the particle at the surface to be unable to rotate in a zero-gradient rotation.

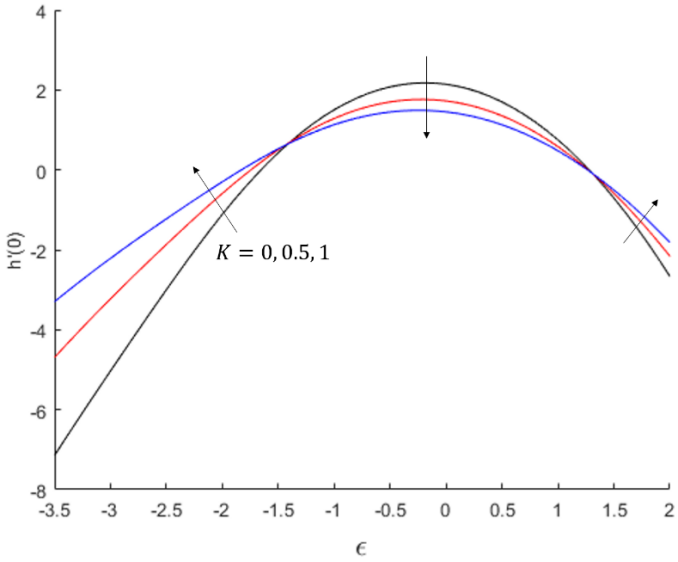

Fig. 3. $M_x \operatorname{Re}_x$ for varies of *K*

Figure 4 indicates that when the plate is subjected to shrinking, the local Nusselt number decreases. The decrease in the local Nusselt number suggests reduced heat transfer efficiency in shrinking flows. This behavior could be due to reduced flow area, leading to lower convective heat transfer rates. For stretching flows, the local Nusselt number shows an increasing trend. However, there is a specific point on the graph where the local Nusselt number increases for the stretching plate but with a relatively minor change compared to other points. It indicates that while stretching flows generally enhance heat transfer, there is a particular region where the improvement is less pronounced.

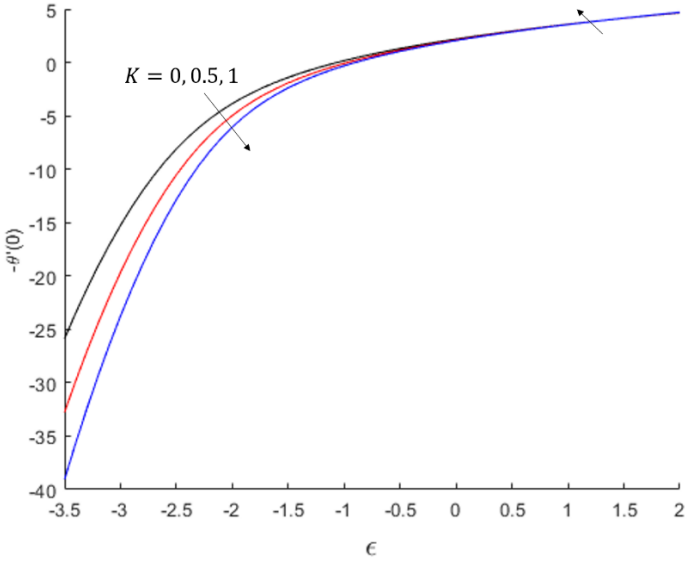

Fig. 4. $Nu_x \left(\operatorname{Re}_x\right)^{1/2} \sqrt{2L / x}$ for varies of *K*

Figure 5 illustrates the relationship between the local Sherwood number and the type of flow (stretching or shrinking) under different conditions. It indicates that the local Sherwood number decreases for shrinking flows, possibly due to slower diffusion in the reduced flow area. On the other

hand, the local Sherwood number increases for stretching flows, indicating improved mass transfer efficiency due to enhanced fluid-surface interaction.

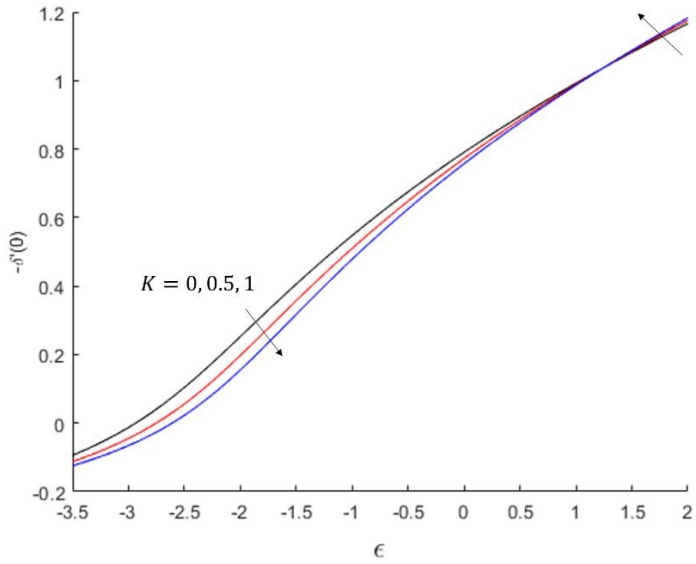

Fig. 5. $Sh_x \left(\mathrm{Re}_x\right)^{1/2} \sqrt{2L / x}$ for varies of *K*

Figures 6-9 show the velocity, angular, temperature, and concentration profiles for various values of K with shrinking plate $\left(\varepsilon = -1\right)$. These profiles asymptotically satisfy the free stream Eq. (11), thus giving us confidence in the accuracy of the current solutions. Figure 6 illustrates the graph's trend of decreasing velocity with increasing micropolar parameters, indicates that these microstructural effects, introduced by the higher micropolar parameter, are causing the fluid to slow down.

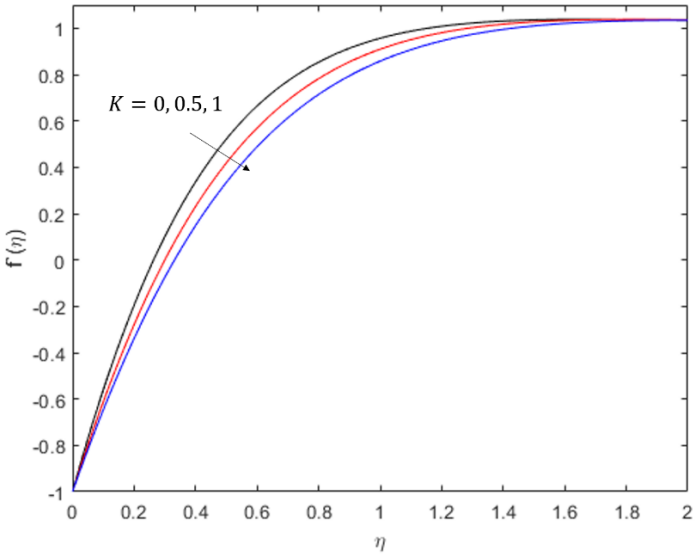

Fig. 6. Velocity Profile for varies of *K*

Figure 7 demonstrates that the angular profile of a specific parameter increases as the micropolar parameter increases. It suggests that higher micropolar parameter values amplify the variations of the measured parameter across different angles or orientations.

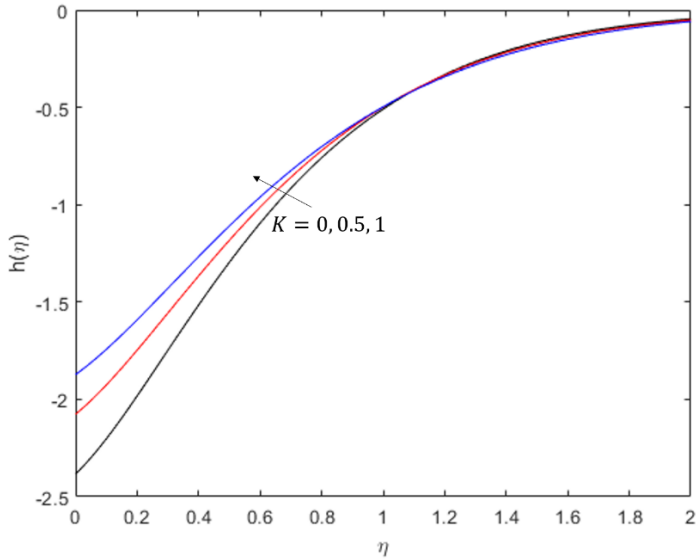

Fig. 7. Angular Profile for varies of *K*

Figure 8 demonstrates that the temperature profile of the fluid increases as the micropolar parameter increases. It indicates that higher micropolar parameter values enhance the thermal behavior of the fluid, resulting in higher temperatures across the surface being measured.

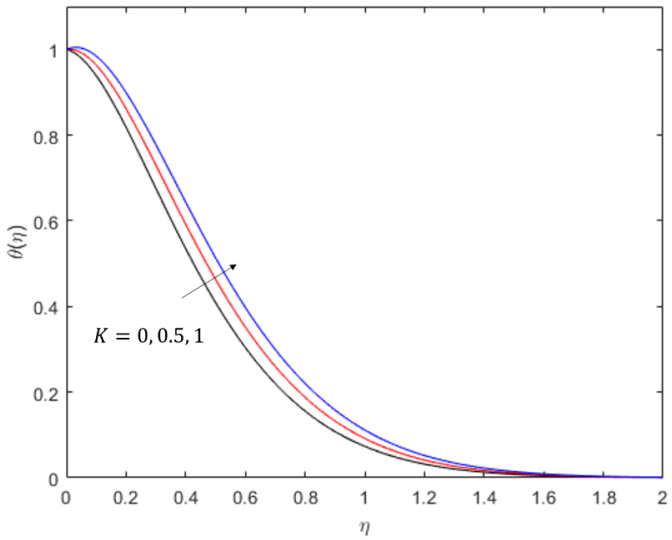

Fig. 8. Temperature Profile for varies of *K*

In Figure 9, a particular substance's micropolar parameter and concentration profile increase. It means that when the micropolar parameter is higher, the behavior of the substance's concentration becomes more pronounced. As a result, higher concentrations across the surface being studied can be observed.

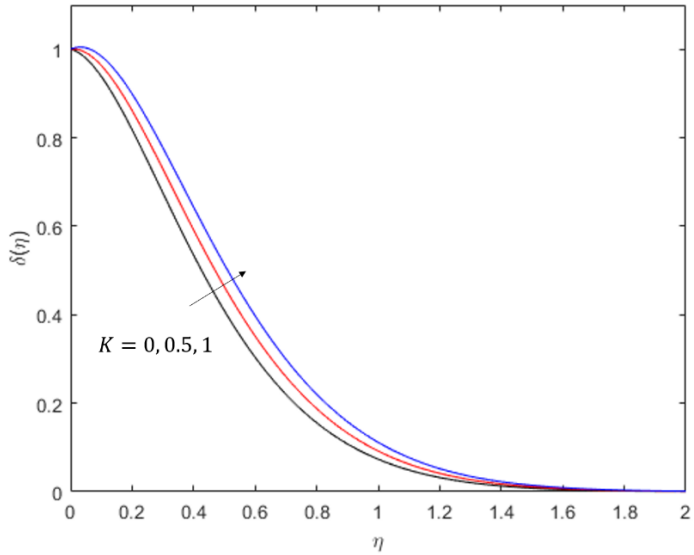

Fig. 9. Concentration Profile for varies of *K*

The effects of α on the $C_f \left(\mathrm{Re}_x\right)^{1/2} \sqrt{2L/x}$, $M_x \mathrm{Re}_x$, $Nu_x \left(\mathrm{Re}_x\right)^{1/2} \sqrt{2L/x}$, and $Sh_x \left(\mathrm{Re}_x\right)^{1/2} \sqrt{2L/x}$ are presented in Figures 10-13, respectively for varies values of $\alpha = 0, \pi/6, \pi/3$. The angles of the plate considered are 0 (horizontal), $\pi/6$ (approximately 30 degrees), and $\pi/3$ (approximately 60 degrees). It can be seen that the skin friction decreases as the angle of the plate increases in Figure 10. It also shows a decrease in skin friction for stretching and shrinking. Additionally, the graph indicates a consistent trend of decreasing skin friction for both stretching and shrinking flows, regardless of the plate's angle. These trends collectively suggest that inclined plates experience reduced skin friction, and stretching and shrinking flows contribute to lower skin friction coefficients.

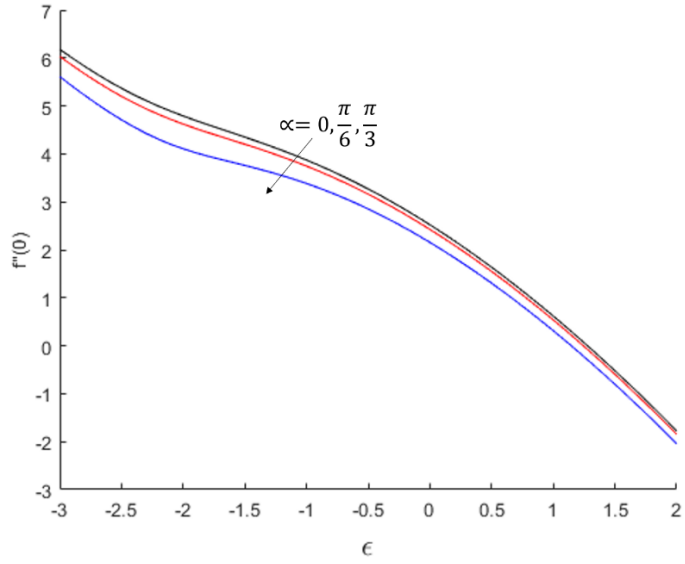

Fig. 10. $C_f \left(\mathrm{Re}_x\right)^{1/2} \sqrt{2L/x}$ for varies of α

Figure 11 illustrates that the local couple stress decreases as the angle of the plate parameter decreases for stretching and shrinking. However, it also shows that the local couple stress values are higher for stretching flows compared to shrinking flows, regardless of the plate's angle. The trend of decreasing local couple stress with plate angle suggests that the influence of couple stresses decreases as the plate becomes horizontal.

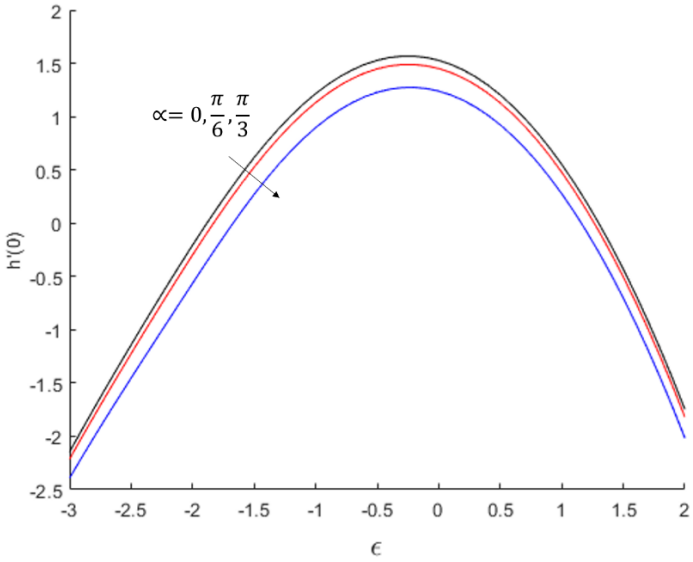

Fig. 11. $M_x \operatorname{Re}_x$ for varies of α

Figure 12 shows that the local Nusselt number decreases as the angle of the plate parameter decreases for stretching and shrinking plate. In addition, decreasing the local Nusselt number with plate angle suggests reduced heat transfer efficiency as the plate becomes horizontal. Furthermore, the enhancement in heat transfer efficiency from shrinking to stretching conditions indicates that stretching the plate improves heat transfer.

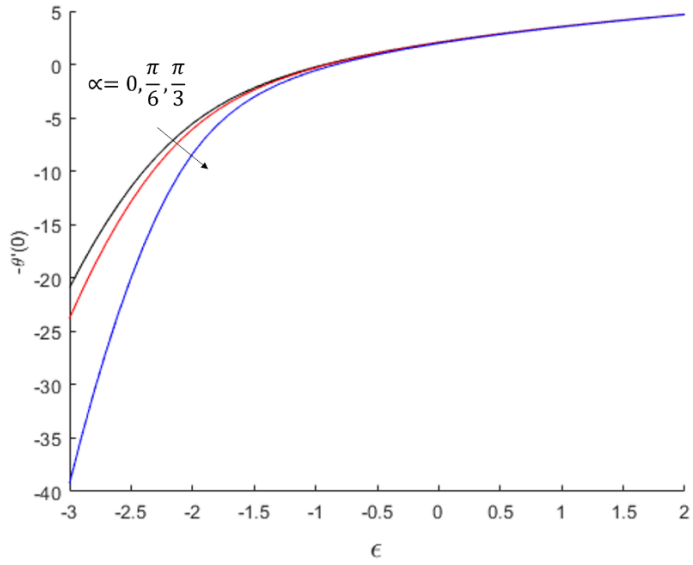

Fig. 12. $Nu_x \left(\operatorname{Re}_x\right)^{1/2} \sqrt{2L/x}$ for varies of α

Figure 13 demonstrates that the local Sherwood numbers decrease as the angle of the plate parameter decreases. It shows that the values of the local Sherwood number increase from shrunk to stretch. The decreasing local Sherwood number with plate angle suggests reduced mass transfer efficiency as the plate becomes horizontal. Furthermore, the enhancement in mass transfer efficiency from shrinking to stretching conditions indicates that stretching the plate improves mass transfer.

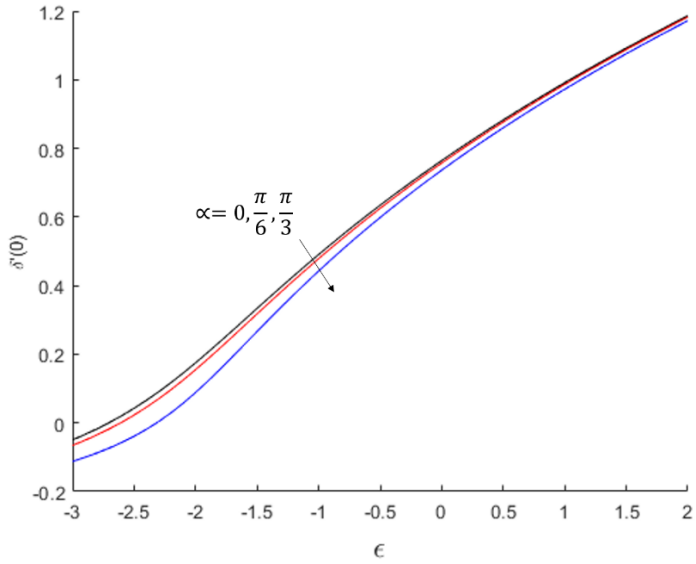

Fig. 13. $Sh_x \left(\mathrm{Re}_x\right)^{1/2} \sqrt{2L / x}$ for varies of α

Figure 14-17 shows the velocity, angular, temperature and concentration profiles for various values of α . In Figure 14, the velocity decreases as the angle of the plate parameter decreases. It indicates that the fluid flows more slowly as the plate becomes horizontal. The decreasing velocity trend with plate angle suggests that the fluid experiences reduced flow speed as the plate angle decreases.

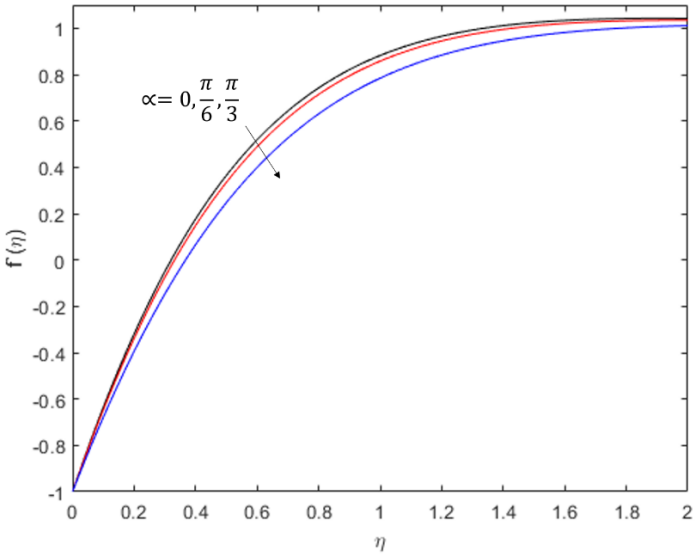

Fig. 14. Velocity profile for varies of α

Figure 15 illustrates that a specific parameter's angular profile increases as the plate parameter's angle increases. It indicates that the variations in the parameter's values across different angles become more pronounced as the plate becomes inclined. The trend of increasing angular profile with plate angle suggests that the orientation of the plate influences the parameter's behavior.

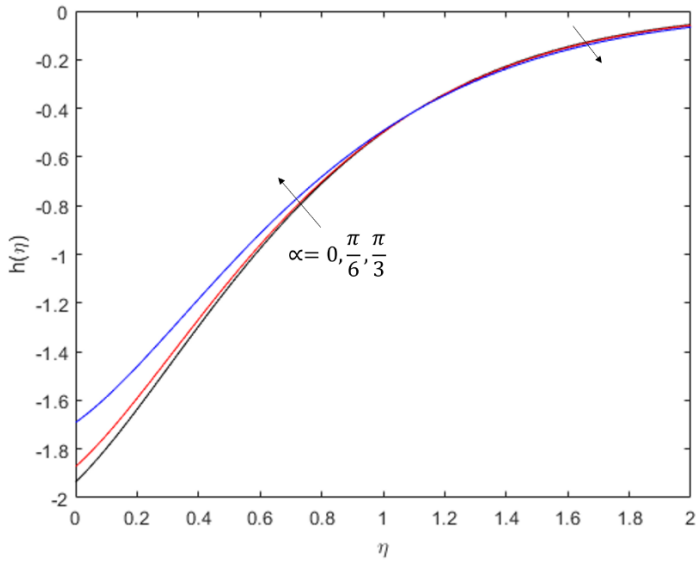

Fig. 15. Angular profile for varies of α

The temperature profile is shown in the Figure 16. It demonstrates that the temperature profile increases due to increases in the angle of the plate parameter. It suggests that more inclined angles of the plate result in higher temperatures across the region or surface of interest. The trend of increasing temperature profile with plate angle indicates that the plate's orientation influences the fluid's thermal behavior.

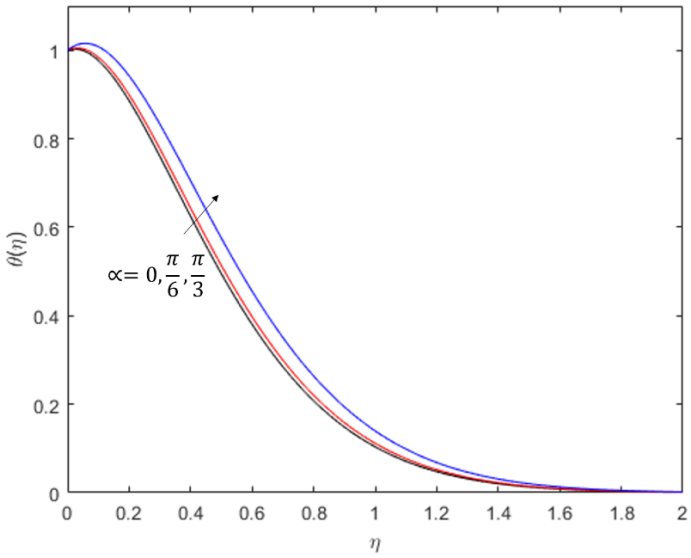

Fig. 16. Temperature profile for varies of α

Figure 17 illustrates that a specific substance's concentration profile increases as the plate parameter angle increases. It indicates that the substance's concentration becomes more

pronounced across the region or surface of interest as the plate becomes inclined. The trend of increasing concentration profile with plate angle suggests that the plate's orientation impacts the distribution of the substance's concentration.

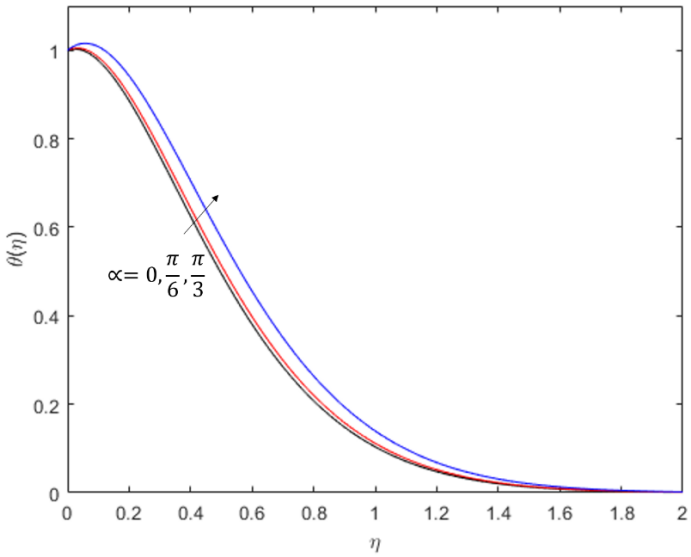

Fig. 17. Concentration profile for varies of α

4. Conclusion

The present study has accomplished a stagnation-point flow and heat transfer over an exponentially stretching/shrinking inclined plate with radiation, MHD, and concentration. The governing equations have been transformed using similarity transformation, which the BVP4c solver solves in Matlab. Some parameters are being considered in this study: the micropolar parameter K , angle of the plate α , stretching/shrinking ε , and other constant parameters to determine the behavior of the $C_f \left(\mathrm{Re}_x\right)^{1/2} \sqrt{2L/x}$, $M_x \mathrm{Re}_x$, $Nu_x \left(\mathrm{Re}_x\right)^{1/2} \sqrt{2L/x}$, $Sh_x \left(\mathrm{Re}_x\right)^{1/2} \sqrt{2L/x}$, as well as the velocity, temperature, and concentration profiles, respectively. The results obtained are as follows:

i. A more significant micropolar parameter decreases the skin friction on shrinking plates and increases it on stretching plates. Otherwise, it leads to higher local couple stress. Shrinking leads to decreased local Nusselt number, indicating reduced heat transfer efficiency, and stretching enhances heat transfer, with a specific point showing minor improvement. Local Sherwood number increases for stretching, suggesting improved mass transfer efficiency.
ii. Increasing the micropolar parameter decreases velocity, possibly due to microstructural effects. Angular profile increases, enhancing variations across angles. Temperature profile increases, indicating enhanced thermal behavior. The concentration profile increases, resulting in more pronounced substance distribution.
iii. Inclined plates experience reduced skin friction. Stretching flows have higher local couple stress than shrinking flows. Local Nusselt number decreases with decreasing plate angle. Stretching flows enhance heat transfer, with a specific point showing minor improvement. Local Sherwood number increases for stretching flows, suggesting improved mass transfer efficiency.

iv. Velocity decreases as plate angle increases, indicating slower fluid flow for more horizontal plates. Angular profile increases with plate angle, indicating more vital variations across different orientations. Temperature and concentration profiles increase with plate angle, influencing thermal behavior and substance distribution.

Acknowledgment
This research was funded by a grant from the Ministry of Higher Education of Malaysia (FRGS/1/2021/STG06/UITM/02/11).

References

[1] Soid, Siti Khuzaimah, Anuar Ishak, and Ioan Pop. "MHD stagnation-point flow over a stretching/shrinking sheet in a micropolar fluid with a slip boundary." *Sains Malaysiana* 47, no. 11 (2018): 2907-2916. https://doi.org/10.17576/jsm-2018-4711-34

[2] RamReddy, Chetteti, and Teegala Pradeepa. "Spectral quasi-linearization method for homogeneous-heterogeneous reactions on nonlinear convection flow of micropolar fluid saturated porous medium with convective boundary condition." *Open Engineering* 6, no. 1 (2016). https://doi.org/10.1515/eng-2016-0015

[3] Eringen, A. Cemal. "Theory of micropolar fluids." *Journal of mathematics and Mechanics* (1966): 1-18. https://doi.org/10.1512/iumj.1967.16.16001

[4] Ishak, Anuar, Yian Yian Lok, and Ioan Pop. "Stagnation-point flow over a shrinking sheet in a micropolar fluid." *Chemical Engineering Communications* 197, no. 11 (2010): 1417-1427. https://doi.org/10.1080/00986441003626169

[5] Norzawary, Nur Hazirah Adilla, Siti Khuzaimah Soid, Anuar Ishak, Muhammad Khairul Anuar Mohamed, Umair Khan, El-Sayed M. Sherif, and Ioan Pop. "Stability analysis for heat transfer flow in micropolar hybrid nanofluids." *Nanoscale advances* 5, no. 20 (2023): 5627-5640. https://doi.org/10.1039/D3NA00675A

[6] Nazar, Roslinda, Norsarahaida Amin, Diana Filip, and Ioan Pop. "Stagnation point flow of a micropolar fluid towards a stretching sheet." *International Journal of Non-Linear Mechanics* 39, no. 7 (2004): 1227-1235. https://doi.org/10.1016/j.ijnonlinmec.2003.08.007

[7] Ishak, A., R. Nazar, and I. Pop. "Mixed convection stagnation point flow of a micropolar fluid towards a stretching sheet." *Meccanica* 43 (2008): 411-418. https://doi.org/10.1007/s11012-007-9103-5

[8] Borrelli, Alessandra, Giulia Giantesio, and Maria Cristina Patria. "Numerical simulations of three-dimensional MHD stagnation-point flow of a micropolar fluid." *Computers & Mathematics with Applications* 66, no. 4 (2013): 472-489. https://doi.org/10.1016/j.camwa.2013.05.023

[9] Mohammed Alshehri, Ahmed, Hasan Huseyin Coban, Shafiq Ahmad, Umair Khan, and Wajdi Mohamad Alghamdi. "Buoyancy effect on a micropolar fluid flow past a vertical Riga surface comprising water-based SWCNT–MWCNT hybrid nanofluid subject to partially slipped and thermal stratification: Cattaneo–Christov model." *Mathematical Problems in Engineering* 2021 (2021): 1-13. https://doi.org/10.1155/2021/6618395

[10] Mini, Gopinathan Sumathi, Prathi Vijaya Kumar, and Shaik Mohammed Ibrahim. "Numerical Computation of Radiative MHD Micropolar Nanofluid Flow over a Stretching Sheet with First Order Chemical Reaction and Soret Effects." *Journal of Advanced Research in Fluid Mechanics and Thermal Sciences* 108, no. 2 (2023): 77-97. https://doi.org/10.37934/arfmts.108.2.7797

[11] Ferdows, Mohammad, M. D. Shamshuddin, and Khairy Zaimi. "Dissipative-radiative micropolar fluid transport in a nondarcy porous medium with cross-diffusion effects." *CFD Letters* 12, no. 7 (2020): 70-89. https://doi.org/10.37934/cfdl.12.7.7089

[12] Khan, Ansab Azam, Khairy Zaimi, Suliadi Firdaus Sufahani, and Mohammad Ferdows. "MHD Mixed Convection Flow and Heat Transfer of a Dual Stratified Micropolar Fluid Over a Vertical Stretching/Shrinking Sheet With Suction, Chemical Reaction and Heat Source." *CFD Letters* 12, no. 11 (2020): 106-120. https://doi.org/10.37934/cfdl.12.11.106120

[13] Sheikholeslami, M., M. Hatami, and D. D. Ganji. "Micropolar fluid flow and heat transfer in a permeable channel using analytical method." *Journal of Molecular Liquids* 194 (2014): 30-36. https://doi.org/10.1016/j.molliq.2014.01.005

[14] Bhattacharyya, Krishnendu, Swati Mukhopadhyay, and G. C. Layek. "Slip effects on boundary layer stagnation-point flow and heat transfer towards a shrinking sheet." *International Journal of Heat and Mass Transfer* 54, no. 1-3 (2011): 308-313. https://doi.org/10.1016/j.ijheatmasstransfer.2010.09.041

[15] Dzulkifli, Nor Fadhilah, Norfifah Bachok, Nor Azizah Yacob, Ioan Pop, Norihan Arifin, and Haliza Rosali. "Stability solution of unsteady stagnation-point flow and heat transfer over a stretching/shrinking sheet in nanofluid with slip velocity effect." *CFD Letters* 14, no. 1 (2022): 66-86. https://doi.org/10.37934/cfdl.14.1.6686

[16] Japili, Nirwana, Haliza Rosali, and Norfifah Bachok. "Slip effect on stagnation point flow and heat transfer over a shrinking/stretching sheet in a porous medium with suction/injection." *Journal of Advanced Research in Fluid Mechanics and Thermal Sciences* 90, no. 2 (2022): 73-89. https://doi.org/10.37934/arfmts.90.2.7389

[17] Ismail, Nurul Syuhada, Yong Faezah Rahim, Norihan Md Arifin, Roslinda Nazar, and Norfifah Bachok. "Stability analysis of the stagnation-point flow and heat transfer over a shrinking sheet in nanofluid in the presence of MHD and thermal radiation." *Journal of Advanced Research in Fluid Mechanics and Thermal Sciences* 91, no. 2 (2022): 96-105. https://doi.org/10.37934/arfmts.91.2.96105

[18] Vishalakshi, Angadi Basettappa, Ulavathi Shettar Mahabaleshwar, and Giulio Lorenzini. "An Unsteady Hiemenz Stagnation Point Flow of MHD Casson Nanofluid Due to a Superlinear Stretching/Shrinking Sheet with Heat Transfer." *J. Adv. Res. Flud. Mech. Therm. Sci.* 95 (2022): 1-19. https://doi.org/10.37934/arfmts.95.2.119

[19] Waini, Iskandar, Anuar Ishak, and Ioan Pop. "Hybrid nanofluid flow towards a stagnation point on an exponentially stretching/shrinking vertical sheet with buoyancy effects." *International Journal of Numerical Methods for Heat & Fluid Flow* 31, no. 1 (2021): 216-235. https://doi.org/10.1108/hff-02-2020-0086

[20] Uddin, Md Sharif, Krishnendu Bhattacharyya, and Sharidan Shafie. "Micropolar fluid flow and heat transfer over an exponentially permeable shrinking sheet." *Propulsion and Power Research* 5, no. 4 (2016): 310-317. https://doi.org/10.1016/j.jppr.2016.11.005

[21] Rehman, Fiaz Ur, Sohail Nadeem, Hafeez Ur Rehman, and Rizwan Ul Haq. "Thermophysical analysis for three-dimensional MHD stagnation-point flow of nano-material influenced by an exponential stretching surface." *Results in physics* 8 (2018): 316-323. https://doi.org/10.1016/j.rinp.2017.12.026

[22] Soid, Siti Khuzaimah, Siti Nor Asiah Ab Talib, Nur Hazirah Adilla Norzawary, Siti Suzilliana Putri Mohamed Isa, and Muhammad Khairul Anuar Mohamed. "Stagnation Bioconvection Flow of Titanium and Aluminium Alloy Nanofluid Containing Gyrotactic Microorganisms over an Exponentially Vertical Sheet." *Journal of Advanced Research in Fluid Mechanics and Thermal Sciences* 107, no. 1 (2023): 202-218. https://doi.org/10.37934/arfmts.107.1.202218